

simple cases where the dominant loss in the plasma is by volume recombination. The only exception is neon-argon which gave an experimental response whose variation from simple theory is qualitatively predictable.

The values of the ion generation rate and the electron density obtained in these experiments, using a moderate neutron flux from a research reactor, encourage us to believe that fission-fragment-ionization of mixed noble gas systems will find application in nuclear thermionic energy converters. This concept is attractive as a possible alternative to the more usual cesium converter

system because noble gases have a lower electron-neutral atom scattering cross section, are noncorrosive, and can be used with a relatively low temperature emitter.

ACKNOWLEDGMENT

The authors wish to acknowledge gratefully many stimulating discussions with Professor David J. Rose of the Massachusetts Institute of Technology during these investigations.

Electronic Properties of Titanium Monoxide*

STEPHEN PAUL DENKER

Department of Electrical Engineering, Columbia University, New York, New York

(Received 8 February 1965)

Electric, magnetic, and optical properties of the rocksalt form of titanium monoxide ($\text{TiO}_{0.86}$ to $\text{TiO}_{1.25}$) have been studied. TiO is metallic, exhibiting weak paramagnetism. Properties of TiO-phase samples are determined primarily by the relative concentration of titanium and oxygen atoms and to a lesser extent by sample preparation. The resistivity of TiO₁ can be represented as the sum of an extremely large residual resistivity and a temperature-dependent part having positive slope. Although off-stoichiometric samples exhibit resistivity vs temperature variation not typical of metals, the entire phase can be characterized as metallic. Specular reflectance data suggest that the yellow color of TiO-phase samples is due to a plasma edge relaxation in the yellow region of the visible spectrum.

INTRODUCTION

TITANIUM monoxide (TiO) contains a high equilibrium concentration of randomly distributed vacancies in the titanium and oxygen sublattices^{1,2} and has a broad region of chemical and structural homogeneity. The total concentration of lattice vacancies is independent of composition and at ideal stoichiometry about 15% of both atomic sites are vacant.³ Attention was focused on the defective, cubic (NaCl-type) monoxide, which when prepared by rapid cooling from the melt or quenching annealed specimens from above 1225°K, is stable indefinitely at room temperature. By avoiding higher temperatures and making various experiments on the same samples, the composition and structure of each could be expected to remain constant throughout the research. At high temperatures, grain structure and chemical changes have been observed.^{4,5} In general, measurements were confined to room temperature and below because high temperatures would make samples unsuitable for further study.

* Part of this paper is based on a thesis submitted by the author for the degree of Ph.D. in Electrical Engineering at the Massachusetts Institute of Technology.

¹ P. Ehrlich, *Z. Elektrochem.* **45**, 362 (1939).

² S. Andersson, B. Collén, U. Kuylenstierna, and A. Magneli, *Acta Chem. Scand.* **11**, 1641 (1957).

³ S. P. Denker, *J. Phys. Chem. Solids* **25**, 1397 (1964).

⁴ A. D. Pearson, *J. Phys. Chem. Solids* **5**, 316 (1958).

⁵ M. G. McLaren, Rutgers University, Ph.D. thesis (University Microfilms, 1962).

MATERIALS PREPARATION

TiO-phase oxides were prepared by reduction of titanium dioxide with titanium metal. In the initial step of preparing suitable TiO samples, a button arc melter was used. Hardpressed pellets (6000 psi) of pure titanium dioxide⁶ were placed in water-cooled copper hearths together with a stoichiometric amount of massive pure titanium.⁷ The system was filled with argon to a pressure of about 0.5 atm. A charge in one hearth, consisting of titanium metal alone, was melted first to getter the system. In other hearths, titanium melted in the arc reacted quickly with the dioxide to form TiO. The product was turned over and remelted several times to ensure homogeneity. This method yields polycrystalline samples of high density. Although the molten material was in direct contact with the water-cooled copper hearth, no contamination of the melt was detected by spectrographic analysis. Use of a water-cooled copper hearth and tungsten electrode prevents any diffusion of impurities into the melt, because the molten material does not wet the hearth. A fine black powder, an evaporated deposit from the melted ingot, always found on the hearth after melting, also prevented adherence of molten material to the hearth.

⁶ Supplied by the National Lead Company, South Amboy, New Jersey.

⁷ Iodide-process titanium supplied by the Foote Mineral Company, Philadelphia, Pennsylvania.

Arc-melted buttons were then zone melted into long rods in an rf induction furnace.⁸ The TiO charge lay in a crucible, consisting of several parallel small-diameter water-cooled copper tubes, enclosed in an evacuated Vycor tube. The crucible was moved horizontally through the coil of a 465-kHz rf generator. No contamination from the copper was detected and, as with the arc melter, a fine black powder was deposited on the crucible. Rods prepared in this furnace, about 13 cm in length and one-half cm in diameter, were cut lengthwise into four sections and served as the raw charge for an electron-beam floating-zone melter. Their surfaces were extremely clean.

Electron-beam melting was done in a vacuum of 10^{-6} mm Hg, with the tungsten electron gun at -1000 V and sample at ground potential. The gun was raised at a rate of 5 mm/min. The resultant sample had a uniform circular cross section, was polycrystalline but with good average orientation between grains, had few pores, high density, and very large grain size. Electron-beam melted samples were chemically homogeneous. A series of electron-beam melted rods with titanium-to-oxygen ratios ranging from $\text{TiO}_{0.95}$ to $\text{TiO}_{1.30}$ were prepared. Attempts to grow single crystals were unsuccessful. The rapid traverse speed required by this technique and the phase transformation at ca. 1225°K were believed responsible for the failure. All samples were radiographed and several small cracks and tungsten inclusions were found. Portions containing such inclusions or cracks were discarded.

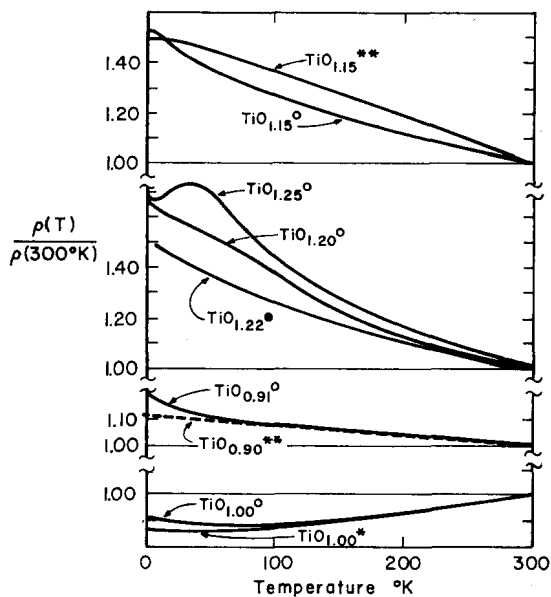


FIG. 1. Comparative plots of the normalized resistivity $\rho(T)/\rho(300^\circ\text{K})$ for TiO-phase samples vs temperature. * arc-melted and annealed at 1030°C . ** sintered. \circ Electron-beam, zone-melted. \bullet Single crystal.

⁸ A. Berghezan and E. Bull-Simonsen, *Trans. AIME* 221, 1029 (1961).

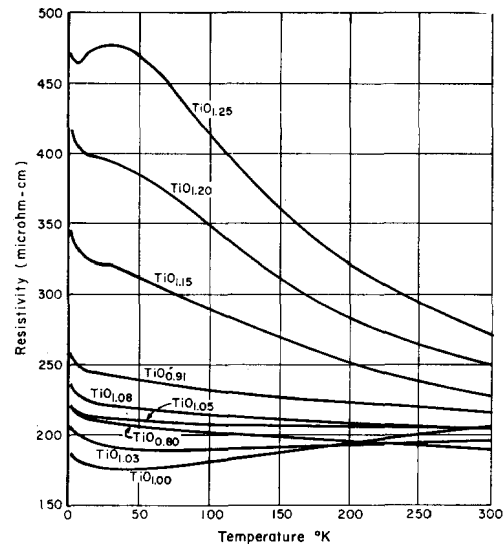


FIG. 2. Low-temperature (1.5° to 300°K) resistivity of electron-beam, zone-melted TiO-phase samples.

X-ray and pycnometric studies of electron-beam melted samples were made; only the lines of the NaCl-type structure were observed. The lattice parameters agreed with published values.² Oxygen determination in TiO samples was made by establishing the weight difference between the initial sample and that obtained after conversion to the highest oxide, TiO_2 .⁹ Several samples were analyzed more than once to check consistency. Nitrogen analysis was made by the Kjeldahl technique and carbon analysis by combustion and conductometric analysis. Spectrographic analyses were also made.¹⁰

Some TiO_1 samples originally prepared by Pearson⁴ by arc melting and annealing were used to study the effects of annealing on electrical properties. Analysis for oxygen content indicated that these samples were very close to ideal stoichiometry TiO_1 .

EXPERIMENTAL RESULTS

Resistivity

Resistivity was measured to three significant figures, sufficient for the observed variations, on a four-terminal 18-Hz ac bridge.¹¹ Maximum sensitivity of the bridge was one microhm. A sample holder was lowered into a wide-neck liquid-helium storage Dewar. The temperature gradient within the neck provided variation in ambient temperature and the helium gas present served to establish thermal equilibrium quickly. A copper-constantan thermocouple with its reference junction in the stored liquid was used. Below 100°K ,

⁹ M.I.T. Laboratory for Insulation Research Progress Report 32, 11 (January 1963).

¹⁰ M.I.T. Laboratory for Insulation Research Progress Report 31, 8 (July 1962).

¹¹ M.I.T. Laboratory for Insulation Research Progress Report 29, 39 (July 1961).

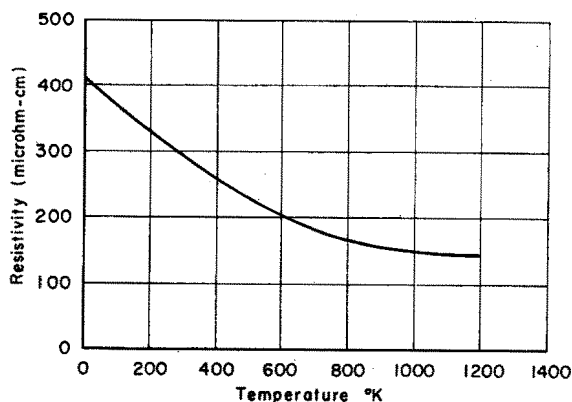


Fig. 3. Resistivity of $\text{TiO}_{1.22}$ single crystal vs temperature.

temperature increments between measurements were approximately 2° to 5°K .

Samples prepared by four different techniques: arc melting plus annealing, sintering, electron-beam zone melting, and arc fusion were investigated (Figs. 1 and 2). Except for the latter sample (Fig. 3) all samples were polycrystalline. For chemically homogeneous samples, the functional dependence of the resistivity vs temperature curves depends primarily on oxygen content (i.e., the value of x in the chemical formula TiO_x) and slightly on method of sample preparation (Fig. 1) in disagreement with McLaren's results.⁵ Photomicrographs⁵ show his samples were poorly sintered, having large pores and not homogeneous. Furthermore, he failed to analyze for actual oxygen content, citing only as-mixed values. Data in Fig. 1 on single crystal oxygen rich, arc melted and annealed, and sintered samples correspond closely to the results obtained on electron-beam melted samples (Fig. 2). The trend in resistivity is clearly evident in Fig. 2. On both sides of ideal stoichiometry the observed slope for the resistivity is negative, while in the region close to the composition TiO_1 it has a positive slope.

Low-temperature resistivities (Fig. 4) of several stoichiometric polycrystalline arc-melted TiO samples prepared and annealed by Pearson⁴ at various temperatures above and below the transformation temperature, were found by this author to exhibit similar temperature dependence with respect to slope and shape. The temperature-dependent part, above 30°K , fits the Grüneisen law (Table I). The curves do show one major difference: as annealing temperature is lowered, the residual resistivity is also reduced. If the low-temperature phase of TiO is primarily an ordering of vacancies in the defective NaCl-type structure, the ordering by reducing the scattering power of the vacancies reduces the residual resistance. In all cases the temperature-dependent part of the resistivity is typically metallic.

The temperature variation of the resistivity of an electron-beam zone-melted sample with composition TiO_1 (Fig. 2) also agreed with the Grüneisen law. Here

TABLE I. Electrical resistivity coefficients for stoichiometric TiO .

Method of preparation	Characteristic temperature θ_R ($^\circ\text{K}$)	Characteristic resistivity $\rho(\theta_R)$ ($\mu\Omega\cdot\text{cm}$)
arc melted and annealed at 846°C	410	215
arc melted and annealed at 900°C	415	181
arc melted and annealed at 960°C	390	220
arc melted and annealed at 1030°C	350	80
Electron beam, zone melted	430	54

the temperature-dependent part of the resistivity was one to two orders of magnitude larger than for typical alkali or noble metals but close to that reported for transition metals, in particular titanium.¹² Two rods of $\text{TiO}_{1.05}$ were electron-beam zone melted (all melting accomplished in 10^{-6} mm Hg vacuum or better) and upon analysis were found to differ in oxygen content by less than two percent. Accuracy of oxygen determinations was about two percent. For this reason, the differences in resistivities of TiO_1 presented in Fig. 4 are believed not to be due to changes in chemical composition but to ordering of lattice vacancies. All electron-

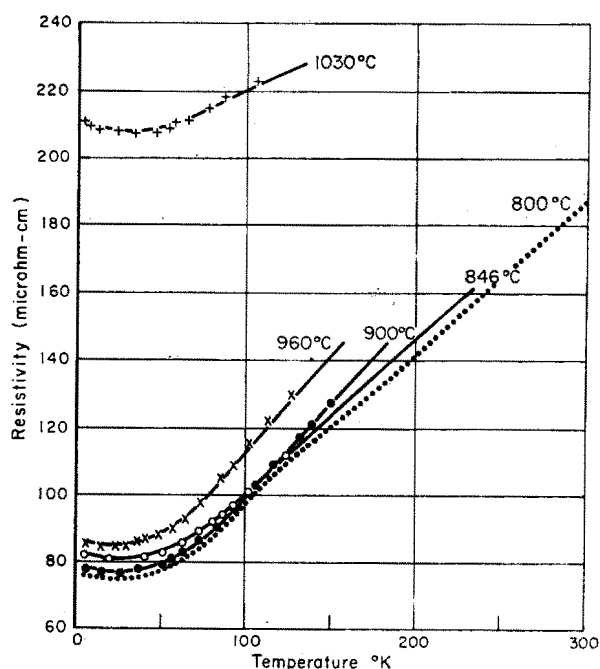


Fig. 4. Low-temperature (4.2° to 300°K) resistivity of arc-melted stoichiometric (TiO_1) samples annealed at different temperatures and quenched.

¹² G. K. White and S. B. Woods, *Phil Trans. Roy. Soc. London* **251A**, 273 (1959).

beam zone-melted TiO-phase samples prepared by the author were found to have the NaCl-type structure.

The resistivity vs temperature data on a $\text{TiO}_{1.22}$ single crystal¹³ was extended to 1200°K (Fig. 3), supplementing the low-temperature data given in Fig. 1. The variation of resistivity does not fit the Grüneisen law, the slope remaining negative to high temperatures. The sign of the relative thermoelectric power remained negative over the entire range investigated.

The off-stoichiometric samples (TiO_x , $0.8 < x < 1.25$, $x \neq 1$) have negative slopes and their behavior stands in marked contrast to that of stoichiometric samples, which have a positive temperature slope of resistivity. If the off-stoichiometric behavior were due only to changes in carrier concentration, then TiO_1 alone could be classified as metallic. However, specular reflectivity and Hall effect data give strong evidence that the carrier concentration is large and virtually independent of temperature. In fact, what is really meant by "metal" is not adherence to the Grüneisen law; the Grüneisen law impules a particular type of charge-carrier scattering by acoustic phonons. The properties that make metals what they are are their high carrier concentration, nearly free-electron mass, and degenerate Fermi statistics. Experimental results indicate that in this sense the entire TiO phase is metallic, and the observed differences in slopes of the resistivity vs temperature data are due largely to the temperature variation of the carrier relaxation time.

There appear, in some samples showing a positive slope in the resistivity vs temperature characteristics (Figs. 2 and 4), resistance minima at low temperatures. No systematic study of the resistance minima was carried out; however, spectroscopic analyses for iron content of two stoichiometric samples exhibiting minima were made. An arc-melted sample (prepared by Pearson⁴ and annealed at 800°C) showing a small minimum (Fig. 4) was found to have ca. 50 ppm iron, while an electron-beam zone-melted sample (prepared by the author) showing a somewhat larger effect (Fig. 2) was found to have an iron content of ca. 200 ppm. These effects, in copper and gold, are caused by spin-dependent scattering due to the presence of extremely small concentrations (as low as 10 ppm) of ferromagnetically

TABLE II. Conductivity and reflectance-minima data for TiO_x .

Sample	Temperature (°K)	Electrical conductivity ($\Omega^{-1} \text{cm}^{-1}$)	λ_{min} (μ)
$\text{TiO}_{1.22}$	300	3500	0.335
$\text{TiO}_{1.22}$	77	2650	0.310
$\text{TiO}_{1.22}$	4.2	2450	0.310
$\text{TiO}_{1.00}$	300	5250	0.325
$\text{TiO}_{1.00}$	77	11 100	0.315
$\text{TiO}_{1.00}$	4.2	13 250	0.320

¹³ Supplied by the Linde Company, East Chicago, Indiana.

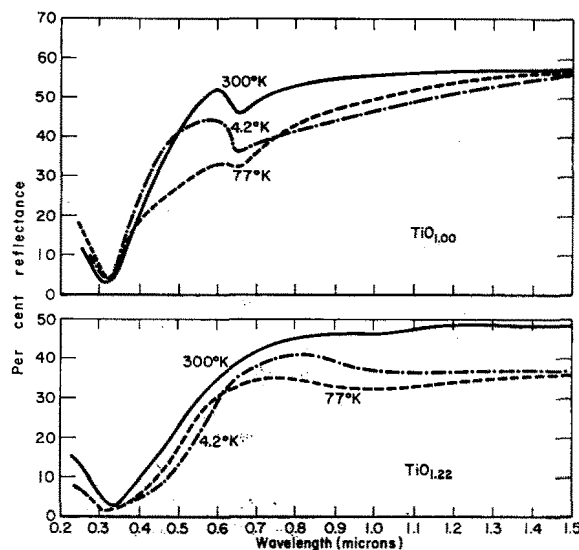


FIG. 5. Specular reflectivity, normal incidence.

coupled paramagnetic impurities, particularly iron.^{14,15} The resistance minimum, if it is due to localized spins,¹⁵ might also be due to uncompensated spins on the randomly disordered vacant titanium sites.

Specular Reflectivity

Reflectivity data (0.2 to 3μ) were taken with a Beckman recording spectrophotometer, model DK, at 4.2°, 77°, and 300°K. Cryostat construction¹⁶ permitted calibration of the room-temperature reflectance amplitude by comparison with a reference standard, but not at liquid-nitrogen or helium temperatures. The latter reflectances may be in error by 20 percent. In all cases the accuracy in wavelength was within one percent.

The specular reflectivity data in Fig. 5 can be used to study the temperature variation of the carrier concentration, by noting the temperature variation of λ_{min} , the wavelength for minimum reflectance, and relating it to the temperature variation of the plasma edge.¹⁷ Furthermore, Kramers-Kronig analysis of these data enables direct evaluation of the real and imaginary parts of the dielectric constant, ϵ_1 and ϵ_2 , and calculation of the energy loss function $-\text{Im}[\epsilon^{-1}]$,^{18,19} and the plasma frequency ω_p .

If the plasma frequency ($\omega_p^2 = Ne^2/m^* \epsilon_0$) relaxation time product $\omega_p \tau > 0$, small changes in carrier concen-

¹⁴ A. V. Gold, D. K. C. MacDonald, W. B. Pearson, and I. M. Templeton *Phil. Mag.* **5**, 765 (1960).

¹⁵ J. Kondo, *Progr. Theoret. Phys. (Kyoto)* **32**, 37 (1960).

¹⁶ The reflectometer and cryostat assembly were designed by Dr. A. Linz, Massachusetts Institute of Technology, Cambridge, Massachusetts.

¹⁷ The plasma is the collection of unbound charge carriers in a partially filled band.

¹⁸ H. R. Philipp and H. Ehrenreich, *Phys. Rev.* **129**, 1550 (1963).

¹⁹ The complex dielectric constant $\epsilon = \epsilon_1 + i\epsilon_2$ and $-\text{Im}[\epsilon^{-1}] = -\text{Imaginary Part of } 1/\epsilon = \epsilon_2/(\epsilon_1^2 + \epsilon_2^2)$.

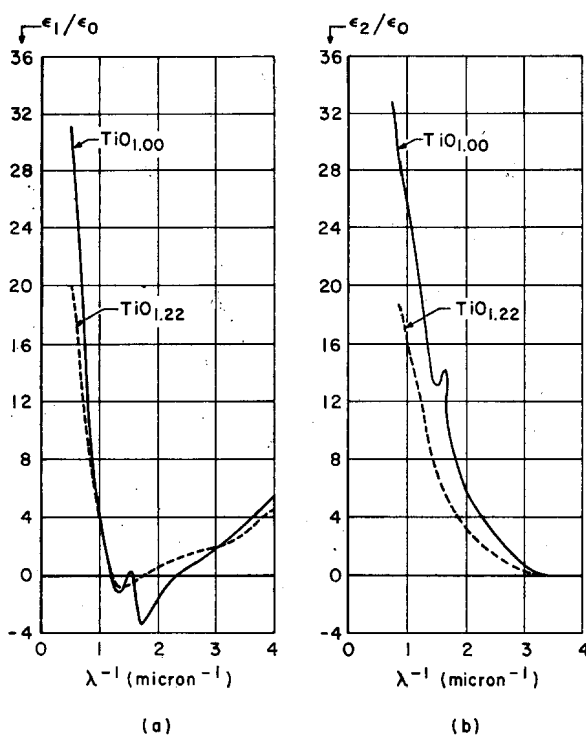


FIG. 6. Relative dielectric constant, at room temperature, obtained from Kramers-Kronig analysis of specular reflectance data. (a) Real part ϵ_1/ϵ_0 . (b) Imaginary part ϵ_2/ϵ_0 .

tration will cause noticeable plasma wavelength shifts. Near ω_p , the index of refraction n is²⁰

$$n^2 \approx \epsilon_1/\epsilon_0 \approx \epsilon_\infty/\epsilon_0 [1 - (\omega_p/\omega)^2], \quad (1)$$

(where ϵ_∞ is the dielectric constant contributed by polarization sources other than unbound charge carriers; ω is the frequency of electromagnetic radiation) and the specular reflectance for normal incidence

$$R \approx 100(n-1)^2/(n+1)^2. \quad (2)$$

The frequency $\omega = \omega_{\min}$ for which R is minimum ($n=1$) is related to ω_p ($n=0$) by

$$\omega_p^2 = \omega_{\min}^2 (1 - \epsilon_0/\epsilon_\infty) = Ne^2/m^* \epsilon_\infty. \quad (3)$$

Finite electrical conductivity means some loss must occur so the minimum reflectance actually is ca. 1 to 5%.

Reflectivity data on two samples: an arc-melted polycrystalline sample TiO_1 annealed at 800°C , and a single crystal $\text{TiO}_{1.22}$ are summarized in Table II. We note that the position of the observed plasma edge appears to account for the yellow color of titanium monoxide. In the infrared region (1 to $3\ \mu$), the reflectance at room temperature was greater for $\text{TiO}_{1.00}$ with its larger dc electrical conductivity than for $\text{TiO}_{1.22}$ in agreement with theory.²⁰ In this spectral region:

$$100 - R \sim (\sigma)^{-1/2}, \quad (4)$$

²⁰ F. Seitz, *Modern Theory of Solids* (McGraw-Hill Book Company, Inc., New York, 1940), pp. 638-642.

TABLE III. $N/m^* \epsilon_\infty \equiv N^*$ as a function of λ_{\min} for $\text{TiO}_{1.00}$ and $\text{TiO}_{1.22}$.

$\text{TiO}_{1.22}$	$N^*_{77^\circ}/N^*_{300^\circ} = N^*_{4.2^\circ}/N^*_{300^\circ} = (335/310)^2 = 1.17$
$\text{TiO}_{1.00}$	$N^*_{77^\circ}/N^*_{300^\circ} = (325/315)^2 = 1.06$
	$N^*_{4.2^\circ}/N^*_{300^\circ} = (325/320)^2 = 1.03$

where R is the reflectance in percent.²⁰ Using the room-temperature values obtained at $1.5\ \mu$ we obtain:

$$\sigma_{\text{TiO}_{1.00}}/\sigma_{\text{TiO}_{1.22}} = 5250/3500 = 1.5 \quad (5)$$

and

$$(100 - R_{\text{TiO}_{1.22}}/100 - R_{\text{TiO}_{1.00}})^2 = (52/43)^2 = 1.47. \quad (6)$$

The small temperature dependence of $N/m^* \epsilon_\infty$ (Table III) from 4.2° to 300°K suggests that the observed variation in resistivity for TiO -phase samples is caused by changes in the carrier relaxation time.

Since the room-temperature specular reflectance is within 5%, we can use it together with the Hall coefficient (Table IV²¹⁻²³) to determine the relative dielectric constant of the solid $\epsilon_\infty/\epsilon_0$ and ω_p , and also to calculate the effective mass m^* , carrier mobility μ , and relaxation time τ presented in Table V. The required information is obtained by the use of a Kramers-Kronig integral which enables evaluation of the complex dielectric constant $\epsilon(\omega) = \epsilon_1 + i\epsilon_2$ given in Fig. 6.²⁴ The energy loss function $-\text{Im}[\epsilon^{-1}]$ given in Fig. 7 has a maximum at the plasma resonance and ω_p can be calculated to order $1/\omega_p^2 \tau^2$. The plasma frequency can also be obtained from the relationship $\epsilon_1 = 0$, see Eq. (1), but in contrast that value obtained above agrees with the plasma frequency only to lower order.¹⁸ The relaxation time τ appearing in the electrical conductivity, $\sigma = Ne^2 \tau / m^*$, which is assumed also to describe the lifetime of the plasma oscillations, can be estimated from the total width of the peak in $-\text{Im}[\epsilon^{-1}]$ at half the maximum.¹⁸ The experimentally observed widths $\Delta\omega/\omega = 2/\omega_p \tau$ are in good agreement with the values of τ obtained from σ .

TABLE IV. Hall coefficient of titanium monoxide (n -type).

T (°K)	Composition	Reference	Hall coefficient (m^3/C)
300°	$\text{TiO}_{1.00}$	21	$-(5.3 \pm 0.5) \times 10^{-10}$
	$\text{TiO}_{1.00}$	22	$-(1.5 \pm 0.1) \times 10^{-10}$
	$\text{TiO}_{1.19}$	23	$-(2.08 \pm 0.6) \times 10^{-10}$
77°	$\text{TiO}_{1.22}$	22	$-(0.70 \pm 0.05) \times 10^{-10}$
	$\text{TiO}_{1.00}$	22	$-(1.5 \pm 0.1) \times 10^{-10}$
4.2°	$\text{TiO}_{1.22}$	22	$-(1.05 \pm 0.15) \times 10^{-10}$
	$\text{TiO}_{1.22}$	22	-1.6×10^{-10}

²¹ A. A. Samokhvalov and A. G. Rustamov, *Soviet Phys.—Solid State* **5**, 877 (1963).

²² J. Piper, Union Carbide Research Institute, Tarrytown, New York (private communication).

²³ W. A. Navipour, Massachusetts Institute of Technology, SM thesis (1959), unpublished.

²⁴ J. M. Ballantyne, M.I.T. Laboratory for Insulation Research Technical Report **189**, (May 1964), pp. 33-37.

TABLE V. Transport parameters for TiO_{1.00} and TiO_{1.22}.

	T (°K)	ω_p (rad/sec)	$\epsilon_\infty/\epsilon_0$	m^*/m_0	τ (sec)	$(\text{cm}^2/\text{V}\cdot\text{sec})$
TiO _{1.00}	300	5.2×10^{15}	2.5	2.0	0.9×10^{-15}	0.80
	77	5.2×10^{15}	2.5	2.0	0.9×10^{-15}	0.80
TiO _{1.22}	300	4.5×10^{15}	1.6	8.5	1.2×10^{-15}	0.25
	77	4.5×10^{15}	1.6	6.0	0.85×10^{-15}	0.25
	4.2	4.5×10^{15}	1.6	3.5	0.8×10^{-15}	0.40

This interpretation is valid since $\omega_p\tau \approx 5$, which is sufficient to satisfy the original assumption $\omega_p\tau > 1$ and agrees with the low values for the observed reflectance at λ_{min} .

Absolute Thermoelectric Power

The thermoelectric power was measured at room temperature²⁵ and the raw data were corrected by measuring the relative thermoelectric power of pure lead, whose absolute thermoelectric power is known.²⁶

The absolute thermoelectric power at room temperature (Fig. 8) was generally negative in sign throughout the TiO phase. With the exception of TiO_{0.8}, compositions within the TiO phase had negative absolute thermoelectric powers.

The thermoelectric power for arc-melted and annealed stoichiometric samples is affected strongly by residual resistivity contributions. As the residual resistivity decreases the thermoelectric power decreases. In metals where the residual resistivity $\Delta\rho$ is high, the thermoelectric power will include an additive term of²⁷

$$Q = Q_f \cdot (\rho_L E' + \Delta\rho \Delta E') / (\rho_L + \Delta\rho), \quad (7)$$

where

$$E' = -E_f \cdot [\partial \ln \rho_L / \partial E]_{E=E_f},$$

$$\Delta E' = -E_f \cdot [\partial \ln \Delta\rho / \partial E]_{E=E_f},$$

and $Q_f = -2.45 \times 10^{-2} T / E_f (\mu\text{V}/^\circ\text{C})$ is the absolute thermoelectric power of a free-electron metal, E_f is measured in eV from the conduction band edge, and ρ_L is the temperature-dependent part of the resistivity. E' and $\Delta E'$ will be more or less constant as $\Delta\rho$ changes,

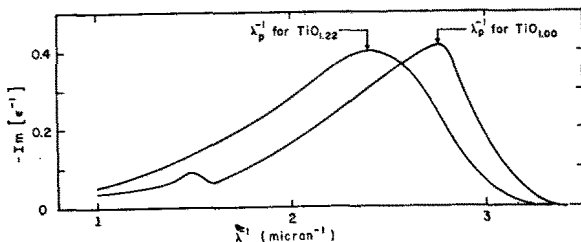


Fig. 7. Room-temperature energy loss function $-\text{Im}[\epsilon^{-1}]$.

²⁵ N. Bobson, Electronics 34, 61 (8 December 1961).

²⁶ J. W. Christian, J. P. Jan, W. B. Pearson, and I. M. Templeton, Proc. Roy. Soc. (London) A245, 220 (1958).

²⁷ J. M. Ziman, Electrons and Phonons (Clarendon Press, Oxford, England, 1960), pp. 400-403.

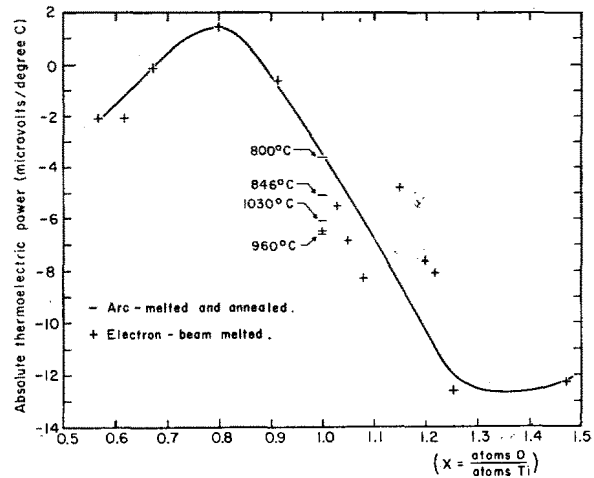


Fig. 8. Absolute thermoelectric power of TiO-phase samples (TiO_x) at room temperature.

even though $\Delta\rho$ may be large compared to ρ_L .²⁷ At all but the smallest values for $\Delta\rho$, Q will be typical of the residual resistivity $Q_f \Delta E'$. Friedel²⁸ finds the measured values of ΔQ are generally negative for alloys containing transition-metal impurities and the temperature variation is given by Q_f .

Magnetic Susceptibility

The magnetic susceptibilities of several TiO-phase samples, given in Table VI, were measured from 77° to 300°K. All samples were found to be weakly paramagnetic, magnetization being linear in the applied magnetic field and slightly dependent on temperature. Susceptibilities on either side of stoichiometry show small positive slopes, whereas at stoichiometry the slope is approximately zero up to 1000°K. The observed behavior is apparently due to Pauli paramagnetism. Deviations from stoichiometry disrupt interatomic bonds and could give an additive term to the susceptibility. The positive slope would parallel the character of the resistivity vs temperature properties of non-stoichiometric samples because at low temperatures conduction carriers can become trapped in unfilled bonds. Since much of the bonding is covalent in nature,³ a trapped carrier will reduce the effective moment at the

TABLE VI. Room-temperature magnetic susceptibility of TiO-phase samples.

Composition	$\chi_p \times 10^{+6}$
TiO _{0.80}	1.3
TiO _{0.91}	1.9
TiO _{1.00}	1.7
TiO _{1.15}	1.2
TiO _{1.25}	1.1

²⁸ J. Friedel, Nuovo Cimento Suppl. 7, 287 (1958).

TABLE VII. Properties of TiO₁ (defective NaCl-type).

Property	Value	Source
<i>n</i> -type, electrons majority carriers		Hall effect, thermoelectric power
Carrier concentration	~1 electron per Ti atom	Hall effect
Effective mass	~2 <i>m</i> ₀	reflectivity and Hall effect
Resistivity (300°K)	200 μΩ·cm	
Relaxation time (300°K)	~10 ⁻¹⁸ sec	
Absolute thermoelectric power (300°K)	-6.5 μV/°C	
Slope of resistivity	positive	
Mobility	~0.8 cm ² /V·sec	
Mean free path	10 Å	
Number titanium atoms/unit cell	3.4	density, x ray
Number titanium atoms/cm ³	4.75 × 10 ²² /cm ³	density, x ray
Color	yellow	reflectivity
<i>N/m</i> [*] independent of temperature		Hall effect and reflectivity

bonding site. As the temperature is increased, trapped carriers are re-excited to the conduction band, and the empty trap reassumes an effective magnetic moment.

The small values for the paramagnetic susceptibility imply that the conduction band is nearly empty or the effective mass is near to the free-electron value. The experimental value for the bulk susceptibility of 1.7×10^{-6} emu/gm for TiO₁, corrected for the diamagnetism of the ionic cores,²⁹ gives for comparison a value ca. 2.05×10^{-6} emu/g. This value is reasonable for a metal exhibiting Pauli paramagnetism.

Summary

Titanium monoxide is metallic, exhibits weak paramagnetism, has high carrier concentration and temperature independent *N/m*^{*}. Although the details of scattering differ from typical metals in certain respects, at stoichiometry Matthiessen's rule and Grüneisen's law seem to be obeyed so the resistivity of TiO₁ can be represented as a sum of a high residual resistivity plus a temperature-dependent part having positive slope. High carrier concentration and temperature independent *N/m*^{*} persists for off-stoichiometric samples and the entire phase can be characterized by degenerate Fermi statistics. The high resistivity of TiO as compared with metals does not appear due to conduction within a single so-called narrow band (with an enormous effective mass *m*^{*}) as proposed by Morin,³⁰ but rather to the large concentration of randomly disordered lattice vacancies.³¹

It is important to know whether the low carrier mobility, $\mu = e\tau/m^*$, means a small τ or a large *m*^{*}. Our

²⁹ J. H. Van Vleck, *Theory of Electric and Magnetic Susceptibilities* (Clarendon Press, Oxford, England, 1932), p. 225.

³⁰ F. J. Morin, *Bell System Tech. J.* **37**, 1047 (1958).

³¹ A study of the influence of carbon vacancies on the residual resistivity of TiC similarly shows a large effect: 16 micron-cm/atomic-percent carbon vacancy. Cf. W. S. Williams, *Phys. Rev.* **135**, A505 (1964).

data interpreted according to standard band theory is summarized in Table VII. These data suggest that the relaxation time is small, whereas the effective mass is not much different from *m*₀. In stoichiometric TiO we would expect electron-phonon scattering to give a typical metallic resistivity vs temperature characteristic. But the high concentration of disordered lattice vacancies gives an extremely large residual resistivity or temperature-independent³² part which dominates the total resistivity at all temperatures.

Pearson⁴ prepared a series of stoichiometric TiO samples annealed above and below the transition temperature (1225°K). The temperature dependence of the resistivity of these samples, measured from 4.2° to 300°K by the present author, is similar. The main difference between them is the low-temperature residual resistance. If the low-temperature phase is primarily a long-range ordering of lattice vacancies, the conductivity of samples annealed at lower temperatures is increased because an ordered arrangement of scattering sites disturbs the conductivity less than the same number of randomly distributed sites would.

Deviation from the ideal stoichiometry provides another scattering mechanism, perhaps not recognized generally. The excess titanium or excess oxygen atoms in the lattice give rise to unfilled or *dangling* bonds which trap current carriers. As the temperature is increased, charge carriers are thermally re-excited into the conduction band. We are thus led to the viewpoint that electrical conduction in off-stoichiometric TiO includes an activated exchange of conduction band carriers with traps produced by decoupled, localized bonds. Such an exchange requires a heat of activation, because of the lattice distortion which surrounds an unpaired bond. The scattering sites are such that the charge carriers are randomly localized on the atomic sites. This trapping mechanism is also consistent with an energy band model which contains states derived both from cation-anion and cation-cation interactions. By disrupting the cation-anion bonding system one introduces localized trapping states into the band which lies close to the Fermi energy and is analogous to the type of localized, *virtual* states proposed by Friedel.²⁸

The proposed trapping mechanism above also predicts an additional effect observable in the bulk magnetic susceptibility. If a sample departs from stoichiometry, and we have a titanium-rich or oxygen-rich composition, the odd or missing titanium atoms decouple the spin system and the susceptibility either side of stoichiometry increases because the titanium 3*d* orbitals have unpaired spins. The spins of orbitals at stoichiom-

³² Because the large vacancy concentration produces regions in which the potential energy fluctuates drastically, the physical situation is much more complicated than any considered in a simple model. Nonetheless, description of transport behavior in terms of a simple metallic model provides a reasonably faithful description of the observed properties.

³³ J. B. Goodenough, *Phys. Rev.* **117**, 1442 (1960).

etry are paired antiparallel so as to maximize orbital overlap thereby reducing the effective moment to negligible value.³³ When $x \neq 1$ (TiO_x , $0.8 < x < 1.25$) the bond system is disrupted giving an additional paramagnetic term which increases with temperature since: (a) more bonds are disordered at higher temperatures; and (b) carriers trapped in vacant bonds, tending to restore antiparallel spin pairing, are thermally excited into the conduction band increasing the susceptibility. The magnetic moment in the TiO phase is still very small and due largely to Pauli paramagnetism of the conduction electrons.

The properties of TiO are determined primarily by the relative concentration of titanium and oxygen atoms and to a lesser extent on sample preparation. Sensitivity to sample preparation is not as great as previously reported.⁵ The negative thermoelectric power, characterizing the TiO phase, is largely due to its high residual resistivity. Experimental evidence suggests that the typically yellow color exhibited by

TiO-phase samples is due to the plasma edge occurring in the yellow region of the visible spectrum. The mechanical properties of TiO are intimately connected with strongly directed covalent bonding. Because titanium comes early in the transition-metal series, considerable orbital overlap is possible, and TiO exhibits metallic conductivity.

The most uncertain transport parameter is the effective mass. Reflectance, Hall effect, and absolute thermoelectric power data are somewhat ambiguous. Experiments which directly study Fermi surface topology would be most illuminating with regard to both electrical and magnetic properties.

ACKNOWLEDGMENTS

The author is especially indebted to Professor D. J. Epstein for his initial guidance of this research, to J. M. Ballantyne for the computer analysis of our reflectance data, and to Dr. J. Piper for the Hall effect measurements.

Electron Emission from Aluminum after Quenching*

R. N. CLAYTOR†, J. E. GRAGG‡, AND F. R. BROTZEN

Rice University, Houston, Texas

(Received 23 July 1965)

Emission of electrons ("Exo-electrons") from aluminum was observed by an openwindow Geiger-Müller counter after quenching from temperatures between 300° and 450°C. Emission rates as a function of time at room temperature agreed well with data calculated on the basis of a model involving the diffusion of point defects toward the surface. The energy of formation for the process was determined and discussed in terms of point imperfections.

INTRODUCTION

ELECTRON emission ("exoelectrons") from metals can be stimulated by abrasion, plastic deformation, particle or photon irradiation, as well as by phase transformations.¹ A number of mechanisms has been proposed to account for this emission. Most of the investigators now agree that the emission requires the formation or the presence of a nonmetallic surface layer. The exact emission process, however, is still not fully understood.

It has been demonstrated that plastic deformation tends to lower the photoemission-threshold fre-

quency.²⁻⁴ Grunberg and Wright,⁵ who found a strong emission peak near a wave length of 4700 Å and a weaker one near 5200 Å in freshly abraded aluminum, attributed the emission to the presence of F' centers in the surface layer. These centers were thought to have formed from vacancy pairs created during deformation.⁶ Several other investigators⁷⁻⁹ were unable to reproduce these results, thereby disputing the validity of Grunberg and Wright's hypothesis.

² W. Edlinger and H. Müller, *Anz. Österr. Akad. Wiss.* **91**, 89 (1954).

³ J. Kramer, *Metalloberfl.* **9**, 1, 28 (1955).

⁴ E. Schmid and K. Lintner, *Anz. Österr. Akad. Wiss.* **92**, 158 (1955).

⁵ L. Grunberg and K. H. R. Wright, *Proc. Roy. Soc. (London)* **A232**, 403 (1955).

⁶ L. Grunberg and K. H. R. Wright, *Acta Phys. Austr.* **10**, 375 (1957).

⁷ B. Sujak, *Phys. Blätter* **15**, 209 (1959).

⁸ P. Petrescu, *Studii Cerc. Fyz.* **11**, 867 (1960).

⁹ M. A. Conrad and S. Levy, *Nature* **189**, 887 (1961).

* Research supported by the U. S. Office of Naval Research under Grant No. 2116(02).

† Present address: Texas Instruments, Inc., Dallas, Texas.

‡ Present address: Northwestern University, Evanston, Illinois.

¹ For a review of the literature on this effect see H. J. Mueller, U. S. Army Engr. R and D. Labs. Res. Rep. 1704-RR (20 Dec. 1961); and L. Grunberg, *Brit. J. Appl. Phys.* **9**, 85 (1958).